MOLECULAR AND CELLULAR BIOLOGY, Nov. 2004, p. 9752–9762 Vol. 24, No. 22
0270-7306/04/$08.00+0 DOI: 10.1128/MCB.24.22.9752–9762.2004

The TBC (Tre-2/Bub2/Cdc16) Domain Protein TRE17 Regulates Plasma Membrane-Endosomal Trafficking through Activation of Arf6†

Lenka Martinu,[1] Jeffrey M. Masuda-Robens,[1]‡§ Sarah E. Robertson,[1]‡ Lorraine C. Santy,[2] James E. Casanova,[2] and Margaret M. Chou[1]*

Department of Cell and Developmental Biology, University of Pennsylvania School of Medicine, Philadelphia, Pennsylvania,[1] and Department of Cell Biology, University of Virginia Health Sciences Center, Charlottesville, Virginia[2]

Received 21 April 2004/Returned for modification 8 June 2004/Accepted 17 August 2004

TBC (Tre-2/Bub2/Cdc16) domains are predicted to encode GTPase-activating proteins (GAPs) for Rab family G proteins. While approximately 50 TBC proteins are predicted to exist in humans, little is known about their substrate specificity. Here we show that TRE17 (also called Tre-2 and USP6), a founding member of the TBC family, targets the Arf family GTPase Arf6, which regulates plasma membrane-endosome trafficking. Surprisingly, TRE17 does not function as a GAP for Arf6 but rather promotes its activation in vivo. TRE17 associates directly with Arf6 in its GDP- but not GTP-bound state. Mapping experiments pinpoint the site of interaction to the TBC domain of TRE17. Forced expression of TRE17 promotes the localization of Arf6 to the plasma membrane, leading to Arf6 activation, presumably due to facilitated access to membrane-associated guanine nucleotide exchange factors (GEFs). Furthermore, TRE17 cooperates with Arf6 GEFs to induce GTP loading of Arf6 in vivo. Finally, short interfering RNA-mediated loss of TRE17 leads to attenuated Arf6 activation. These studies identify TRE17 as a novel regulator of the Arf6-regulated plasma membrane recycling system and reveal an unexpected function for TBC domains.

Vesicular trafficking is controlled by small GTPases of the Rab/Ypt and Arf subfamilies (11, 14, 17, 42, 57). Over 60 Rab and six Arf GTPases have been identified in mammals. In most cases, both dominant negative and constitutively active alleles perturb trafficking, indicating that cycling between the GTP- and GDP-bound state is essential for normal function. Cycling is regulated by guanine nucleotide exchange factors (GEFs), which promote GTP-loading and GTPase-activating proteins (GAPs), which accelerate GTP hydrolysis.

Regulators of the Rab and Ypt GTPases are relatively poorly characterized. Studies of GAPs for Rab/Ypt in *Saccharomyces cerevisiae* have identified a core catalytic domain (63, 66, 69). Based on homology with this domain (3, 39), over 50 Rab GAPs have been predicted to exist in humans (5). The Rab GAP homology domain has alternatively been referred to as the TBC (Tre-2/Bub2/Cdc16) (58), PTM (6, 34, 72), and TrH domain (33, 35). We refer to this domain hereafter as TBC, as this nomenclature is used in the databases. Little is known regarding their substrate specificity, as target GTPases have been identified for only three mammalian TBC proteins, RN-tre, PRC17, and GAP CenA (18, 33, 49). In the current study, we reveal an unexpected role for a TBC domain in regulating an Arf family GTPase.

In contrast to Rabs and Ypts, regulators of Arf GTPases are relatively well characterized, with substrates identified for many (20, 31, 40). For both the GEFs and GAPs, distinct subfamilies have been defined based on the presence of distinct localization motifs, regulatory elements, and catalytic domains (20, 31, 40). This complexity may allow trafficking to be coupled to distinct upstream signaling events at discrete locations in the cell.

Arf6, the most divergent member of the Arf family, regulates trafficking between the plasma membrane and an endocytic compartment (12, 21, 23, 50, 53). While the morphology and cargo of this compartment vary between cell types, Arf6 has a conserved role in regulating the flow of material between this organelle and the plasma membrane (21, 23, 25, 50, 52, 53, 62). In many cells, the Arf6 compartment has a tubular shape and is hence termed the tubular endosome (9, 52-54, 62). Endocytosis through this pathway occurs independently of the classical route requiring clathrin and adaptor protein 2 (53). Furthermore, unique cargo, such as major histocompatibility complex I and β1 integrin, are sorted into Arf6 endosomes. After internalization, Arf6 endosomes can take one of two routes (38): they can fuse with the tubular endosome, followed by recycling of cargo to the plasma membrane, or they can fuse with early endosomes of the classical pathway, followed by targeting of cargo to the lysosome. Inactivation of Arf6 is required for cargo to progress through either of these routes (9). Thus, in cells expressing constitutively active Arf6 (Q67L), membrane is internalized normally, but Arf6 endosomes fail to fuse with the tubular compartment or with classical endosomes. Instead, endosomes and pinosomes induced by acti-

* Corresponding author. Mailing address: University of Pennsylvania School of Medicine, Department of Cell and Developmental Biology, 421 Curie Blvd., BRBII Room 1011, Philadelphia, PA 19104-6160. Phone: (215) 573-4126. Fax: (215) 898-9871. E-mail: mmc@mail.med.upenn.edu.

‡ J.M.M.-R. and S.E.R. contributed equally to this work.

† Supplemental material for this article may be found at http://mcb.asm.org.

§ Present address: Glaxo-IMCB Group Institute for Molecular and Cell Biology, Singapore 117609, Singapore.

vated Arf6 appear to undergo homotypic fusion, leading to the accumulation of large vacuoles and a block in recycling of cargo to the plasma membrane (9).

While plasma membrane recycling through this pathway occurs constitutively, it can also be stimulated by agonists such as epidermal growth factor (30), bombesin (8), colony-stimulating factor (71), scatter factor/hepatocyte growth factor (44), serum, and integrin activation (51). Some of these agonists have been shown to induce GTP loading of Arf6, functioning in part by inducing plasma membrane recruitment of Arf6 GEFs (26, 32, 36, 41, 44, 67, 68). Agonists also induce plasma membrane recruitment of Arf6 by a poorly understood mechanism. Indeed, little is known about the molecular machinery or signaling pathways that regulate trafficking through this pathway.

Rab11 is the only other GTPase that has been shown to be required for recycling from the tubular endosome to the plasma membrane (51). Two additional proteins that appear to regulate this pathway are EHD1 and Gas3/PMP22 (10, 15). Overexpression of EHD1 enhances recycling of cargo to the plasma membrane, while overexpression of Gas3/PMP22 induces morphological alterations in the tubular endosome. The mechanism by which either of these proteins functions is undefined. Aside from these studies, little else is known of how trafficking through the Arf6-dependent plasma recycling system is regulated.

Here, we characterized one of the founding members of the TBC family, TRE17. The TRE17 gene (also referred to as Tre-2 and USP6) was originally identified by virtue of its ability to transform NIH 3T3 cells (37). Recent studies revealed that it also promotes tumorigenesis in humans. The chromosomal translocation t(16;17) (q22;p13) involving the *TRE17* gene was identified as a recurring event in aneurysmal bone cysts, a locally aggressive osseous neoplasm in humans (43). This translocation juxtaposed the highly active promoter of the osteoblast cadherin 11 gene with the entire coding sequence of *TRE17*.

We previously reported that TRE17 encodes a component of a novel effector pathway for the Rho GTPases Cdc42 and Rac1 (34). Localization of TRE17 was controlled by mitogens: upon serum or epidermal growth factor stimulation it was recruited from a tubulovesicular compartment to the plasma membrane. This relocalization was mediated by indirect interaction of TRE17 with activated Cdc42 and Rac1. Because TBC domains encode putative GAPs for Rab GTPases, we predicted that TRE17 might regulate trafficking between the plasma membrane and the tubulovesicular compartment. Surprisingly, we found that the TRE17 TBC domain targets Arf6. Our data indicate that the TBC domain does not encode an active GAP for Arf6 but functions to bind Arf6 specifically in its GDP-bound form. This interaction appears to promote plasma membrane localization of Arf6, facilitating access to its GEFs and leading to activation of Arf6 in vivo. Our studies demonstrate an unexpected function for a TBC domain and identify TRE17 as a novel regulator of Arf6-dependent trafficking.

MATERIALS AND METHODS

Tissue culture. HeLa cells were maintained in Dulbecco's modified Eagle's medium containing 10% fetal bovine serum, penicillin, streptomycin, and fungizone. Transfections were performed with Lipofectamine 2000 (Life Technologies, Inc.) or Fugene (Roche Biochemicals) according to the manufacturer's instructions.

Plasmids and constructs. Arf6 and Arf1 constructs, tagged with hemagglutinin (HA) in pLNCX or untagged in pXS, and Myc-EFA6 were generously provided by Julie Donaldson. TRE17 constructs were subcloned into HA-pcDNA3 or pEGFP-C1; mutants T17(447), TBC, and ΔTBC have been described previously (34).

Antibodies. Anti-HA was purchased from Santa Cruz Technologies and Roche Biochemicals. Anti-Flag was from Sigma, and anti-Myc was from Roche Biochemicals. Anti-Arf6 antibody was generously provided by Julie Donaldson.

Immunofluorescence and immunoelectron microscopy. Immunofluorescence was performed as described (34). Cells were fixed, permeabilized, incubated with primary antibodies, and washed. Samples were incubated with fluorescently labeled secondary antibodies (anti-mouse antibody–indocarbocyanine, anti-rabbit antibody–fluorescein isothiocyanate, or anti-rabbit antibody–indodicarbocyanine), washed, and then mounted with SlowFade (Molecular Probes). For antibody internalization experiments, anti-major histocompatibility complex type I (W6/32), anti-β1 integrin (TS216), or transferrin-Alexa Fluor 488 (Molecular Probes) was added to the medium for 2 to 3 h. Cells were fixed and processed as above. Samples were viewed on a Zeiss 510 laser scanning confocal microscope with a C-Apochromat 63x1.2Wcorr objective, with excitation wavelengths of 488 nm (fluorescein isothiocyanate), 546 nm (indocarbocyanine), or 633 nm (indodicarbocyanine). Images were processed with LSM510 software and Adobe Photoshop.

For immunoelectron microscopy, HeLa cells were transfected with HA-T17(447)/pCDNA, fixed in 0.2% glutaraldehyde, permeabilized in 0.2% saponin, and then incubated with anti-mouse immunoglobulin G conjugated to 1.4-nm gold particles. Samples were then refixed with 0.2% glutaraldehyde and subjected to silver enhancement and osmium treatment.

Coimmunoprecipitation of TRE17 and Arf6. HeLa cells were transfected with Lipofectamine 2000. Cells were lysed in Arf6 lysis buffer (50 mM Tris [pH 7.5], 100 mM NaCl, 2 mM $MgCl_2$, 0.1% sodium dodecyl sulfate, 0.5% sodium deoxycholate, 1% Triton X-100, 10% glycerol, 1 mM dithiothreitol, 1 mM phenylmethylsulfonyl fluoride, 0.7 μg of pepstatin per ml, and 1 μg of leupeptin per ml), then pelleted at 16,000 × *g* for 10 min at 4°C. An aliquot of the clarified supernatant was immunoblotted directly. The remainder was precipitated with glutathione-Sepharose for 4 h at 4°C. Beads were washed three times in Arf6 wash buffer (phosphate-buffered saline, 5 mM $MgCl_2$, 0.5% Triton X-100, 1 mM dithiothreitol, plus protease inhibitors as above), then fractionated by sodium dodecyl sulfate (SDS)–12% polyacrylamide gel electrophoresis (PAGE). The top part of the gel was immunoblotted with anti-glutathione *S*-transferase (GST) to detect TRE17 peptides, the bottom part with anti-HA to detect Arf6.

In vitro binding assays. Plasmids encoding wild-type Arf6 and *N*-myristoyltransferase were cotransformed into *Escherichia coli* BL21. Myristoylated Arf6 was purified as previously described (56). Arf6 isolated in this manner is predominantly GDP bound; this was confirmed with GGA3 pulldown assays (unpublished data). T17(447) and the TBC domain were subcloned into pMAL-C2 and then expressed in BL21. Maltose-binding protein (MBP) fusions were expressed and isolated with amylose resin as described (4). Arf6 was added to MBP, MBP-TBC, or MBP-T17(447) bound to amylose resin in phosphate-buffered saline with 5 mM $MgCl_2$ and 0.5 mg of azolectin per ml. Following incubation for 2 h, samples were washed 3 times in the same buffer, fractionated by SDS–12% PAGE, and immunoblotted with anti-MBP and anti-Arf6. Alternatively, Arf6 was first loaded with GTPγS or GDP in vitro as previously described (22) and then subjected to pulldowns with MBP fusions as above.

GGA3 pulldown assays. Assays to monitor Arf6 activation were performed as described (60). HeLa cells were cotransfected with HA-Arf6 and the indicated plasmid with Lipofectamine 2000. The following day, cells were lysed in Arf6 lysis buffer and pelleted at 16,000 × *g* for 5 min at 4°C. An aliquot of the clarified supernatant was taken directly for immunoblotting. The remainder was incubated with GST-GGA3 (20 to 25 μg) conjugated to glutathione-Sepharose for 30 min at 4°C. Beads were washed three times in 50 mM Tris (pH 7)–100 mM NaCl–2 mM $MgCl_2$–1% NP-40–10% glycerol–1 mM dithiothreitol plus protease inhibitors. Samples were fractionated by SDS–12% PAGE. For assays testing the effects of T17(447) on Arf6, cells were treated with cytochalasin D (200 nM) for 30 min prior to lysis to quiesce Arf6. Previous studies have shown that Arf6 accumulates in its inactive form at the tubular endosome under these conditions (21, 52, 62). Minimal effects on the actin cytoskeleton were observed with this treatment (unpublished data). For the assays examining cooperativity between T17(447) and EFA6, cytochalasin D was not used.

Generation and analysis of TRE17-depleted cells. TRE17 expression was ablated by subcloning 5′-GATCCCCTATGACAAGGGACACCGAG-TTCAA GAGACTCGGTGTCCCTTGTCATATTTTTGGAAAGC-3′ (annealed to its

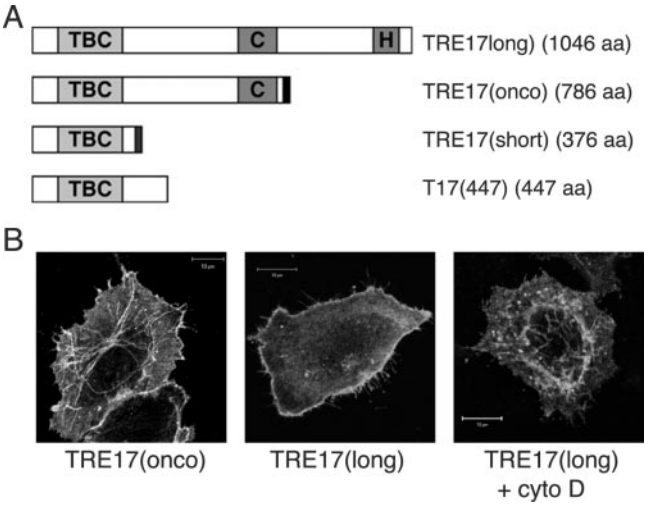

FIG. 1. TRE17 peptides traffic between plasma membrane and tubulo-vesicular compartment. (A) Domain structure of the three TRE17 isoforms TRE17(long), TRE17(onco), and TRE17(short). Also shown is mutant T17(447), encoding amino acids 1 to 447 of TRE17(long). The length of each (in amino acids) is indicated. TBC, Rab GAP homology domain; C and H, cysteine and histidine subdomains of the ubiquitin-specific protease domain, respectively. Dark bars at the C termini of TRE17(onco) and TRE17(short) represent unique sequences. (B) HA-tagged TRE17 isoforms were transfected into HeLa cells, visualized with anti-HA, and analyzed by confocal microscopy. Cells expressing TRE17(long) were treated with cytochalasin D (cyto D, 200 nM) for 30 min (right). Scale bar, 10 μm.

complement) into siRNAneo (provided by Christopher Phiel and Peter Klein, University of Pennsylvania). This construct targets bp 64 to 82 of TRE17. As a negative control, we subcloned 5′-GATCCCCTCGTCAGTGTCAGACACATT AAGCTTGTGTGGTCTG-ACACTGACGATTTTTGGAAAGC-3′ into siRNAneo. This construct targets an exon which is absent from the *TRE17* splice variant expressed in HeLa cells and serves as a control for nonspecific effects of short double-stranded RNA. HeLa cells were transfected with the indicated siRNAneo plasmid with Lipofectamine 2000. The next day, cells were reseeded and supplemented with neomycin (Life Technologies; 800 μg/ml). RNA was isolated after 6 to 7 days, at which time untransfected HeLa cells were killed. RNA was isolated with Trizol (Life Technologies). Reverse transcription-PCR was performed with the ProSTAR HF single-tube system (Stratagene). For amplification of TRE17, the primers were 5′-TGCACTTAAGGTTCAGCAGA A-3′ and 5′-ATGGATCCGTGCTCAAGCAT-3′ ; for glyceraldehyde 3-phosphate dehydrogenase, the primers were 5′-GAGTCAACGGATTTGGTC-3′ and 5′-CCATGCCAGTGAGCTTCC-3′.

For measuring Arf6-GTP levels, neomycin-selected cells were reseeded and cotransfected with HA-Arf6 and the indicated siRNAneo construct. GGA3 pull-down assays were performed as above.

RESULTS

TRE17 localizes to the Arf6-regulated tubular endosome. Three TRE17 isoforms, TRE17(long), TRE17(onco), and TRE17(short), are generated through alternative splicing (37, 48) (Fig. 1A). All three are identical through their amino-terminal 359 amino acids, comprising the TBC domain, but have divergent carboxy termini: TRE17(long) encodes a functional ubiquitin-specific protease (47), consisting of the essential cysteine (Cys) and histidine (His) subdomains (Fig. 1A). TRE17(onco) is identical to TRE17(long) but is truncated following the Cys subdomain. Thus, TRE17(onco) is inactive as a ubiquitin-specific protease (47). Finally, the C terminus of TRE17(short) encodes a unique 17-amino-acid peptide with no additional conserved motifs. Both TRE17(onco) (which was the focus of our previous studies) and TRE17(long) promote tumorigenesis when overexpressed (37, 43). We determined that TRE17(long) is the sole detectable isoform expressed in HeLa cells and the predominant isoform expressed in a variety of adult human tissues and immortalized cell lines (unpublished data). It is therefore the focus of our current studies.

Given its TBC domain, we explored TRE17's role in vesicular trafficking. To identify the compartment in which it functions, we examined TRE17's localization by confocal microscopy. Because none of the five anti-TRE17 antibodies that we generated was sensitive enough for immunofluorescence microscopic detection of endogenous TRE17(long), hemagglutinin epitope-tagged forms of TRE17(long) and TRE17(onco) were transiently expressed in HeLa cells. Consistent with our previous work, HA-TRE17(onco) localized to tubulovesicular structures and the plasma membrane in asynchronously growing cells (Fig. 1B). In contrast, while occasional tubulovesicular staining of HA-TRE17(long) was seen, it was more typically found at the plasma membrane in the majority of cells (Fig. 1B). We had previously shown that tubulovesicular staining of HA-TRE17(onco) was enhanced at the expense of plasma membrane staining by treatment of cells with cytochalasin D (34). Cytochalasin D similarly enhanced tubular staining of HA-TRE17(long) (Fig. 1B). These results suggest that TRE17 peptides traffic between a tubular compartment and the plasma membrane in a manner that depends on F-actin. Furthermore, they suggest that sequences at the C terminus of TRE17(long) may promote its steady-state localization to the plasma membrane.

The enhanced tubular staining of TRE17 upon cytochalasin D treatment was highly reminiscent of what has been described for Arf6 (53). This led us to examine whether the TRE17-positive tubules correspond to the Arf6 tubular endosome. Since Arf6 antibodies did not efficiently detect endogenous Arf6, HA-Arf6 and green fluorescent protein (GFP)-TRE17 were coexpressed in HeLa cells. Under normal conditions (i.e., in the absence of cytochalasin D) Arf6 localized predominantly to vesicles but was occasionally found on tubules (Fig. 2A and 3A), consistent with previous reports (21, 52, 54). As shown in Fig. 2A, GFP-TRE17(onco) colocalized with HA-Arf6 on tubules and vesicles. TRE17(onco) did not enhance the tubular staining of Arf6 or perturb the morphology of the tubular endosome. In contrast, coexpression of TRE17(long) with Arf6 caused dramatic alterations in the morphology of this compartment (see next section).

To confirm that TRE17 peptides localize to the Arf6 tubular endosome, we examined its colocalization with another marker of this compartment. Previous studies have shown that the tubular endosome is enriched in phosphatidylinositol 4,5-bisphosphate, with a GFP-tagged pleckstrin homology (PH) domain from phospholipase Cδ (9). The TRE17(onco) tubules colocalized precisely with GFP-PLCδ(PH) (Fig. 2B). The staining pattern of GFP-PLCδ(PH) was comparable in the absence (Fig. S1 in the supplemental material) or presence of TRE17(onco) coexpression, indicating that TRE17(onco) does not enhance the formation of tubules or perturb the morphology of this compartment. We also confirmed that endogenous cargo of this pathway colocalized with TRE17 (see below). Together, these results demonstrate that TRE17 peptides lo-

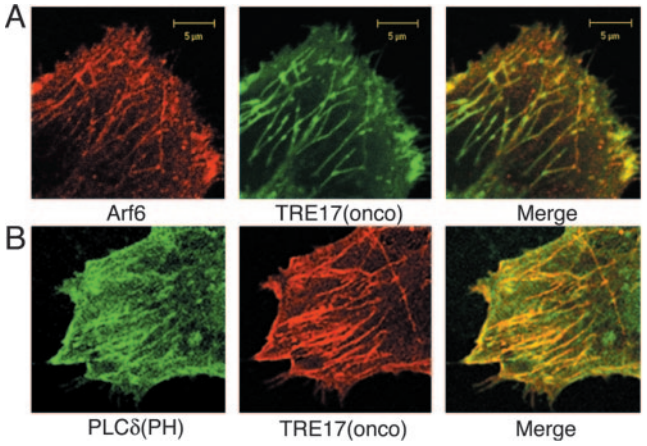

FIG. 2. TRE17 localizes to the Arf6 tubular endosome. HeLa cells were cotransfected with HA-Arf6 (red) and GFP-TRE17(onco) (green) (A) or HA-TRE17(onco) (red) and GFP-PLCδ(PH) (green) (B). Cells were subjected to indirect immunofluorescence with anti-HA antibody and then analyzed by confocal microscopy. Scale bar, 5 μm.

calize to the Arf6-regulated tubular endosome. Because Arf6's role in plasma membrane recycling has been studied most extensively in HeLa cells, we continued our analysis of TRE17 in these cells.

TRE17 induces morphological alterations indicative of Arf6 activation. In examining the colocalization of TRE17(long) with Arf6, we found that this isoform had profound effects on the morphology of the tubular endosome upon coexpression with Arf6. When expressed by itself, Arf6 localized predominantly to the plasma membrane and small vesicles (Fig. 3A). However, coexpression with TRE17(long) induced the formation of large vacuoles on which the two proteins colocalized (Fig. 3B). While this vacuolar morphology was induced in a low percentage (22%) of cells overexpressing wild-type Arf6, this was increased dramatically to 54% in cells coexpressing TRE17(long) and wild-type Arf6 (Fig. 3F). This phenotype is highly reminiscent of that induced by constitutively active Arf6 (Q67L) (Fig. 3C).

Previous studies have shown that the vacuoles induced by Arf6 Q67L are coated with F-actin (Fig. 3C) and accumulate cargo specific to the Arf6 pathway, such as major histocompatibility complex type I (9; unpublished data). We found that the TRE17(long)/wild-type Arf6 vacuoles also accumulated major histocompatibility complex type I and were coated with F-actin (Fig. 3D and E). Vacuoles were never observed in cells expressing TRE17(long) alone, suggesting that the formation of these structures requires a degree of Arf6 activation obtained only upon coexpression with wild-type Arf6.

In addition to the vacuolar morphology described above, a more modest phenotype was observed in a small fraction of cells coexpressing lower levels of TRE17(long) and wild-type Arf6. In these cells, tubular elements of the endosome were still visible, and enlarged vesicle-like structures that were often clustered near the tubules accumulated (Fig. 4A). We surmised that this morphology might also arise from activation of Arf6, since constitutive activation of Arf6 is believed to promote homotypic fusion of endosomes and prevent their fusion with the tubular compartment. We further reasoned that these cells might be more physiological than the vacuolar cells, given the gross morphological alterations in the latter. We therefore searched for TRE17 mutants that gave an enlarged-vesicle phenotype while containing the smallest possible deletion of TRE17(long). This led to identification of T17(447), which encodes the N-terminal 447 amino acids of TRE17(long) (see Fig. 1 for domain structure). T17(447) was able to induce the formation of enlarged vesicle-like structures when expressed by itself (Fig. 4B). In contrast, TRE17(long) was only able to do so when coexpressed with Arf6, suggesting that T17(447) may represent a constitutively active allele. As seen with TRE17(long), T17(447) could also induce the formation of vacuoles when coexpressed with wild-type Arf6 (data not shown).

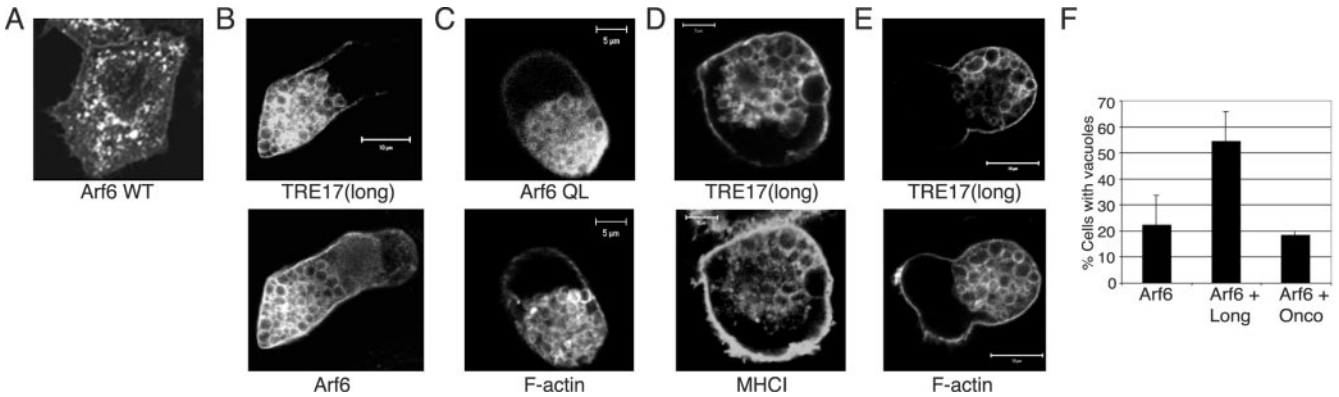

FIG. 3. TRE17(long) and Arf6 cooperate to induce a constitutively active Arf6 phenotype. HeLa cells were transfected with wild-type Arf6 (A) or Q67L (C) and then subjected to indirect immunofluorescence microscopy with anti-Arf6 antibody. For C, F-actin was visualized with fluorescein isothiocyanate-phalloidin (bottom). (B, D, and E), HA-TRE17(long) and wild-type Arf6 were cotransfected. In B, the two proteins were detected with anti-HA and anti-Arf6 antibodies, respectively. (D) Live cells were labeled with anti-major histocompatibility complex type I for 2 h prior to fixation. (E) F-actin was visualized with fluorescein isothiocyanate-phalloidin. Scale bar, 10 μm in A, C, and E; 5 μm in B and D. (F) Cells were transfected with wild-type Arf6 alone or with TRE17(long) or TRE17(onco). Numbers represent the percentage of cells coexpressing Arf6 and the indicated TRE17 peptide that contain vacuoles. The data represent the results of at least three independent experiments in which 100 cells were counted per experiment.

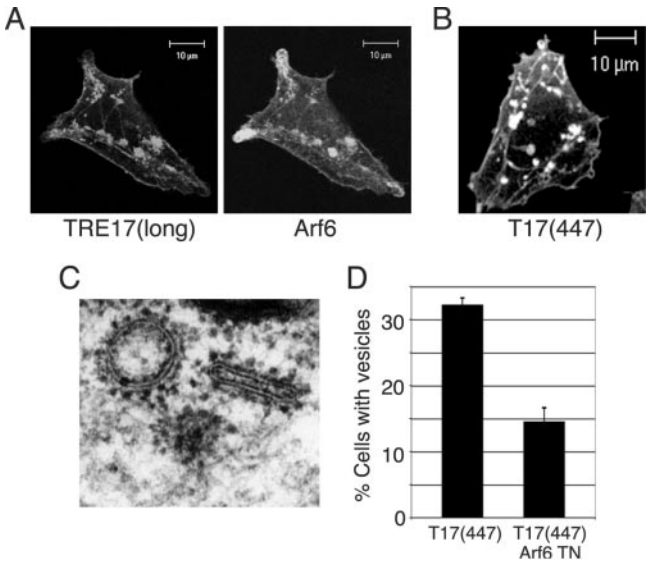

FIG. 4. Alterations in tubular endosome morphology induced by TRE17 arise through activation of endogenous Arf6. HeLa cells were transfected with (A) HA-TRE17(long) and wild-type Arf6 or (B) HA-T17(447), encoding the N-terminal 447 amino acids of TRE17(long) (see Fig. 1 for domain structure) and then analyzed by confocal microscopy. (C) HeLa cells were transfected with HA-T17(447), and immunoelectron microscopy was performed with anti-HA antibody and secondary antibody conjugated to 1.4-nm gold particles. (D) The percentage of HA-T17(447)-expressing cells containing enlarged vesicles (as typified in B) was quantified in the absence and presence of coexpressed Arf6 T27N. The results are representative of three independent experiments in which at least 100 cells were counted per experiment. Scale bar, 10 μm.

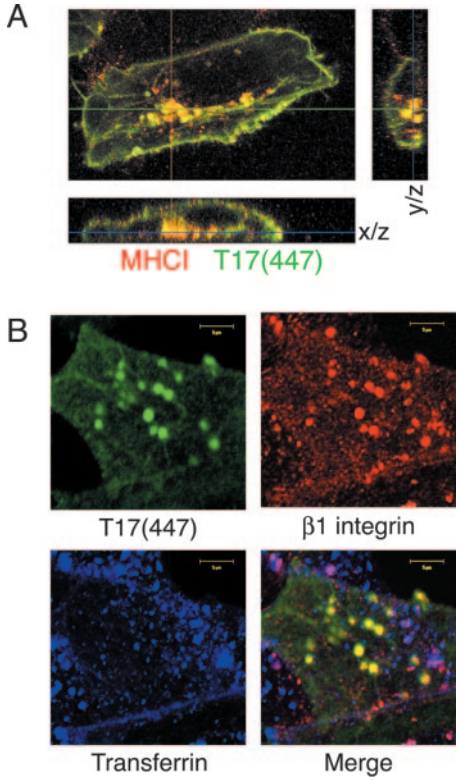

FIG. 5. TRE17 vesicles specifically accumulate cargo of the Arf6 pathway. (A) Live HeLa cells expressing HA-T17(447) were incubated with anti-major histocompatibility complex type I for 2 h. Samples were fixed and subjected to indirect immunofluorescence microscopy, visualizing internalized anti-major histocompatibility complex type I (red) and T17(447) (green). (B) HeLa cells expressing T17(447) (green) were incubated with anti-β1-integrin (red) and Alexa Fluor 488-transferrin (blue) for 2 h prior to fixation. Scale bar, 10 μm.

While the vacuoles induced by coexpression of TRE17(long) or T17(447) with Arf6 precisely phenocopied Arf6 Q67L (regarding molecular markers and morphology), the enlarged vesicle-like structures induced by T17(447) alone had a distinct appearance (compare Fig. 3 and 4). We therefore sought to characterize them further. We first confirmed that these structures were indeed vesicular by performing immunoelectron microscopy. As shown in Fig. 4C, the T17(447)-positive structures were clearly delimited by a membrane bilayer. We next determined whether they arose through activation of endogenous Arf6 by testing whether their formation was blocked by coexpression of dominant negative Arf6 (T27N). While 33% of cells expressing T17(447) alone exhibited enlarged vesicles, as typified in Fig. 4B, this was reduced to 14% in cells coexpressing Arf6 T27N (Fig. 4D). In the remaining cells, vesicles were either absent or greatly reduced in size (data not shown). This result strongly suggests that activation of endogenous Arf6 is required for the ability of T17(447) to induce the formation of enlarged vesicles. In sum, these data provide strong, albeit indirect evidence that TRE17 peptides promote activation of Arf6 in vivo.

TRE17 selectively regulates trafficking of cargo of the Arf6 but not the classical endocytic pathway. We wished to determine the specificity of TRE17's effects on endocytic trafficking. As mentioned above, the Arf6 pathway carries cargo such as major histocompatibility complex type I and β1-integrin but excludes cargo from the classical endocytic pathway, such as the transferrin receptor (9). To assess whether Arf6 cargo selectively accumulated in the T17(447) vesicles, anti-major histocompatibility complex type I, anti-β1-integrin, or fluorescently labeled transferrin was added to the culture medium of transfected HeLa cells and allowed to internalize for 2 h. Cells were then fixed and processed for indirect immunofluorescence. Both anti-major histocompatibility complex type I (Fig. 5A) and anti-β1-integrin (Fig. 5B) were incorporated into the T17(447) vesicles, confirming that they are endocytic in nature. Serial optical sectioning revealed that these structures were clearly inside the cell and not projections from the plasma membrane (Fig. 5A). In striking contrast, transferrin (Fig. 5B) and EEA1 and Rab5 (unpublished data) were excluded from the T17(447) vesicles. Transferrin did colocalize with β1-integrin on a distinct subpopulation of vesicles (Fig. 5B, magenta staining in merge panel), consistent with previous studies showing that endosomes of the Arf6 and classical pathways later fuse (38). These results support the notion that TRE17 selectively regulates trafficking through the Arf6 pathway at a step prior to convergence with the classical pathway.

TRE17 specifically promotes GTP loading of Arf6 in vivo. The morphological studies above suggested that TRE17 promotes activation of Arf6. We wished to confirm this by directly measuring Arf6-GTP levels in vivo. To this end, we used a fragment of the Golgi-localized, γ ear-containing, Arf-binding

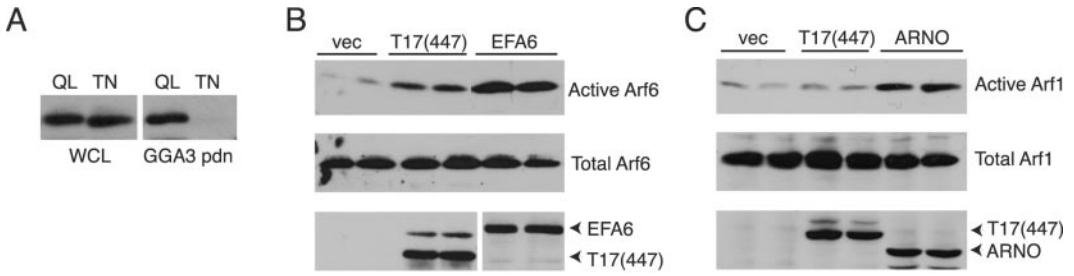

FIG. 6. TRE17 specifically activates Arf6 but not Arf1 in vivo. (A) Extracts were prepared from HeLa cells transfected with HA-Arf6 Q67L or T27N and then subjected to pulldowns (pdn) with GST-GGA3. Arf6 was detected by anti-HA immunoblotting. (B) HA-Arf6 was cotransfected with vector, HA-T17(447), or Flag-EFA6, and GGA3 pulldowns were performed as in A. EFA6 was detected with anti-Flag. Active Arf6, GGA3 pulldowns; total Arf6, whole-cell lysates. (C) HA-Arf1 was cotransfected with vector, HA-T17(447), or Myc-ARNO. GGA3 pulldown assays were performed. ARNO was detected with anti-Myc antibody. Active Arf1, GGA3 pulldowns; total Arf1, whole-cell lysates.

protein GGA3, which binds to Arfs in a GTP-dependent manner (19, 65). GGA3 was purified as a GST fusion from *E. coli* and used as an affinity reagent to pull down active Arf6 from HeLa cell extracts (60). GST-GGA3 pulled down Arf6 Q67L but not T27N (Fig. 6A), demonstrating that it specifically recognizes active Arf6.

We next monitored the effects of T17(447) on Arf6 activity by coexpressing it with wild-type HA-Arf6 and then performing GGA3 pulldowns. Levels of active Arf6 were monitored by anti-HA immunoblotting. Strikingly, Arf6 was potently activated by T17(447) relative to control samples (Fig. 6B). The degree of activation by the Arf6 GEF, EFA6, is shown for comparison. With this assay, Arf6 was not significantly activated by TRE17(long) or TRE17(onco), but this is likely due to the relatively low percentage of cells expressing HA-Arf6 that actually coexpressed these isoforms. In cells on which coexpression was confirmed by immunofluorescence microscopy (as in Fig. 3), TRE17(long) efficiently promoted Arf6 activation, as judged from its ability to mimic the Arf6 Q67L phenotype.

We also monitored the effects of T17(447) on endogenous Arf6 but observed no activation (unpublished data). This is likely due to the technical limitations of this assay, since EFA6 also failed to detectably activate endogenous Arf6. Because the assays above required cotransfection of Arf6, we wished to confirm that T17(447)'s effects were not a consequence of promiscuous activity due to overexpression. We therefore examined activation of another Arf family member, Arf1. HA-Arf1 was coexpressed with T17(447) or ARNO (a GEF for Arf1 and Arf6) (13, 27) and subjected to GGA3 pulldown assays. While ARNO activated Arf1, T17(447) had no effect (Fig. 6C). These results indicate that TRE17 selectively promotes the activation of Arf6 in vivo.

Arf6 binds directly to the TBC domain of TRE17 in a GDP-dependent manner. To better understand the mechanism by which TRE17 promotes Arf6 activation, we examined whether the two proteins associate. GST-TRE17(long) was coexpressed with HA-Arf6 Q67L or T27N. TRE17(long) was precipitated with glutathione-Sepharose, and associated Arf6 was monitored by anti-HA immunoblotting. Surprisingly, TRE17(long) coprecipitated with Arf6 T27N but not Q67L, indicating a GDP-dependent interaction (Fig. 7A). This interaction was highly specific, as no association of TRE17 with Rab4, Rab5, or Rab11 was detected (unpublished data).

To map the Arf6-binding site, mutants of TRE17 (Fig. 7B) were tested for their ability to bind Arf6 T27N. TRE17(onco), T17(447), and the isolated TBC domain coprecipitated with Arf6 T27N as efficiently as TRE17(long) (Fig. 7A). However, a mutant deleted of the TBC domain (ΔTBC) exhibited significantly reduced binding. Thus, the TBC domain of TRE17 is both necessary and sufficient for binding to inactive Arf6 in vivo.

We wished to confirm that TRE17 could also bind to wild-type Arf6 in its GDP-bound state, to exclude the possibility that binding to Arf6 T27N resulted nonspecifically from conformational abnormalities of this mutant. To test this, wild-type Arf6 was cotransfected with T17(447). Cells were treated or not with the glycolytic inhibitor 2-deoxyglucose, which reduces the cellular level of free GTP (61). As seen in Fig. 7C, wild-type Arf6 exhibited a basal association with T17(447) that was further enhanced by 2-deoxyglucose treatment, providing additional evidence for the GDP-dependent association of TRE17 with Arf6 in vivo.

To determine whether this interaction is direct, binding was examined with recombinant proteins. Wild-type Arf6 purified from *E. coli,* which is predominantly GDP bound (56), was incubated with maltose-binding protein (MBP)-tagged T17(447) or the isolated TBC domain conjugated to amylose beads. Arf6 bound to MBP-T17(447) and MBP-TBC but not to MBP alone (Fig. 7D, top panel). To confirm that this interaction was GDP dependent, Arf6 was loaded with GTPγS or GDP prior to incubation with the MBP fusion proteins. As shown in Fig. 7D (bottom panel), Arf6 coprecipitated specifically with the TBC domain in the presence of GDP.

Taken together, our data demonstrate that the TBC domain of TRE17 binds directly to Arf6-GDP. These results were surprising, given that GAP domains interact with GTPases in a GTP-dependent manner and that TBC domains are predicted to interact with Rab GTPases.

TRE17 promotes plasma membrane localization of Arf6 and cooperates with GEFs in Arf6 activation. Given that TRE17 binds to Arf6-GDP and promotes its activation in vivo, we hypothesized that it might function as a GEF. However, we were unable to detect intrinsic GEF activity for recombinant MBP-T17(447) by in vitro GEF assays (unpublished data). We therefore considered alternative mechanisms by which binding of TRE17 with Arf6-GDP might promote its activation.

Arf6-GDP is largely intracellular on tubules and vesicles and

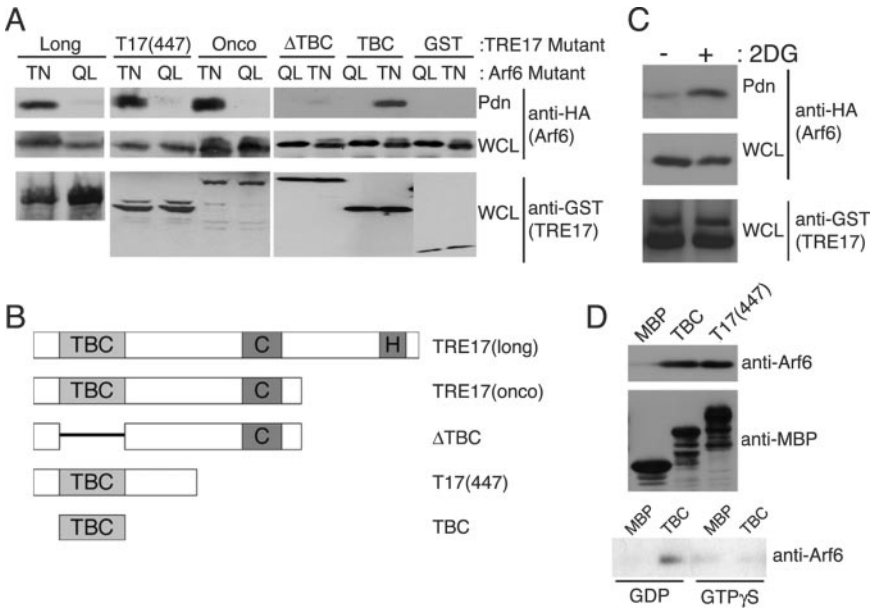

FIG. 7. TBC domain of TRE17 binds directly to Arf6-GDP. (A) HA-tagged Arf6 Q67L (QL) or T27N (TN) was cotransfected with the indicated GST-tagged TRE17 allele into HeLa cells. TRE17 peptides were precipitated with glutathione-Sepharose beads, and associated Arf6 was detected by anti-HA blotting. WCL, whole-cell lysate. Pdn, pulldown. (B) Domain structure of the TRE17 mutants used in A. (C) HeLa cells were cotransfected with GST-T17(447) and wild-type HA-Arf6. Cells were incubated with or without 100 mM 2-deoxyglucose (2DG) for 2 h and then harvested as in A. (D) Purified wild-type Arf6 was incubated with MBP, MBP-TBC, or MBP-T17(447) conjugated to amylose beads. The beads were washed, and the associated Arf6 was detected by anti-Arf6 immunoblotting (top panel); use of comparable levels of MBP fusions was confirmed by anti-MBP blotting (middle panel). In the bottom panel, Arf6 was loaded with GTPγS or GDP in vitro prior to performing pulldowns with MBP or MBP-TBC.

is believed to become activated upon recruitment to the plasma membrane, where Arf6 GEFs reside. We hypothesized that TRE17 might bind to Arf6-GDP at the tubular endosome and promote localization of vesicles to the plasma membrane. To test this, we examined the effects of T17(447) on the localization of Arf6 T27N. Consistent with previous reports (25, 50, 53), Arf6 T27N was predominantly found on vesicles and tubules (Fig. 8A). However in 14% of cells, some plasma membrane staining could be discerned. Coexpression of T17(447) dramatically increased the percentage of cells exhibiting plasma membrane-localized Arf6 T27N to 37% (Fig. 8B). In some cells, Arf6 T27N was almost entirely localized to the plasma membrane (Fig. 8C), a distribution that was never observed in cells expressing Arf6T27N alone. TRE17(long) and TRE17(onco) were also able to enhance plasma membrane localization of Arf6 T27N (Fig. 8D), although the latter did so less efficiently.

Our results suggest that TRE17 peptides function in part by promoting localization of Arf6 to the compartment where its GEFs reside. Thus, one might predict that TRE17 and GEFs would cooperate in Arf6 activation. To test this, levels of transfected EFA6 and T17(447) and EFA6 were titrated down so that modest or no activation by either alone was observed. Strikingly, coexpression of the two at these levels cooperatively activated Arf6 (Fig. 8E). Similar results were obtained with the Arf6 GEF ARNO (Fig. S2 in the supplemental material). These data support a model in which TRE17 functions to facilitate access of Arf6 to its GEFs at the plasma membrane.

TRE17's effects on Arf6 and endosome morphology are independent of intrinsic GAP activity. While our results indicate that TRE17 is not a GAP for Arf6, it remained possible that it might function as a GAP for another GTPase. Indeed, TBC proteins in *Saccharomyces cerevisiae* have been shown to act on multiple GTPases, at least in vitro (1). The only other GTPase reported to localize to the tubular endosomal compartment is Rab11 (51). However, we found that TRE17 neither interacts with Rab11 nor stimulates its GTPase activity (unpublished data).

We considered that TRE17 might function as a GAP for a GTPase that we have yet to identify. To determine whether this putative activity was required for TRE17's effects on Arf6 activation or morphology of the tubular endosome, we generated a mutant that is predicted to be catalytically inactive. TBC domains contain two highly conserved arginine residues that are essential for activity (Fig. 9A, asterisk and arrow). Mutation of either residue in all TBC domain proteins tested thus far renders the enzyme inactive (1–3, 28, 33, 49, 55). The C-terminal arginine residue (arrow, Fig. 9A) functions directly in catalysis and is conserved in GAPs for multiple GTPase subfamilies (5). Strikingly, this position has a threonine (T150) in TRE17, suggesting that it might be catalytically inactive. While the adjacent residue is an arginine (R149), it is likely nonfunctional, based on mutagenic and X-ray crystal structure analysis of other TBC proteins (3, 55). Nevertheless, we entertained the possibility that it might be able to participate in the catalytic mechanism.

To determine whether GAP activity is required for TRE17's effects, we mutated both of the arginines above (arginines 106 and 149) to lysine. This double mutation (RKRK) was made in the context of T17(447) to allow us to monitor its effects on

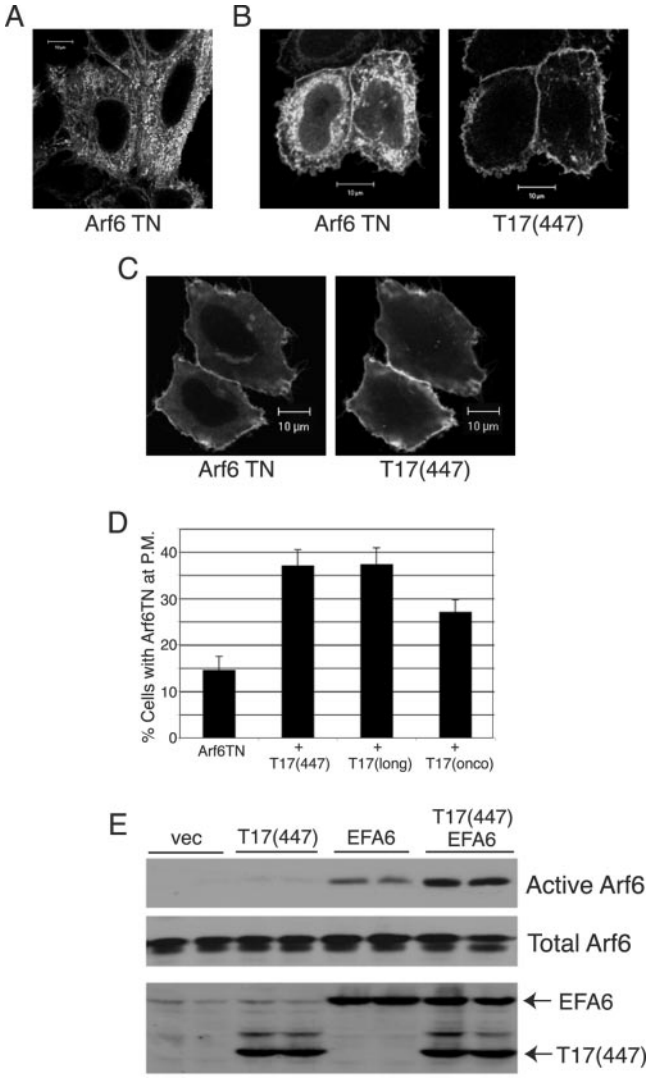

FIG. 8. TRE17 induces plasma membrane recruitment of Arf6 and cooperates with GEFs to promote activation. Arf6 T27N was expressed by itself (A) or with HA-T17(447) (B and C) in HeLa cells. (B) Representative image of plasma membrane-localized Arf6 T27N upon coexpression with T17(447). (C) Complete redistribution of Arf6 T27N to the plasma membrane was observed in a fraction of cells coexpressing T17(447). Scale bar, 10 μm. (D) Arf6 T27N was expressed by itself or with the indicated TRE17 peptide. The percentage of cells exhibiting plasma membrane (P.M.)-localized Arf6 T27N as typified in B was quantified. Results represent three independent experiments in which 100 cells were counted in each. (E) HA-Arf6 was cotransfected with the indicated plasmids into HeLa cells. GGA3 pulldown assays were performed as above.

morphology and Arf6 activation biochemically. RKRK induced the formation of enlarged vesicles that accumulated major histocompatibility complex type I at a frequency indistinguishable from that of wild-type T17(447) (Fig. 9B and data not shown). We next examined whether this mutation perturbed T17(447)'s effects on Arf6. As seen in Fig. 9C and D, T17(447) RKRK activated and associated with Arf6 as well as its wild-type counterpart did in vivo.

These experiments suggest that TRE17's effects on Arf6 activation and tubular endosome morphology do not require intrinsic GAP activity. Further support for this is provided by an experiment in which we attempted to enhance TRE17's potential GAP activity. Since TRE17 lacks the catalytic arginine residue at the conserved position, we reasoned that converting T150 to arginine might render it more active. However, we found that this substitution had no effect on the ability of T17(447) to induce the formation of enlarged vesicles (unpublished data). Thus, while it remains formally possible that TRE17 functions as a GAP for a GTPase that we have yet to identify, our results suggest that this is unlikely. Rather, our data strongly suggest that the TBC domain of TRE17 serves as an Arf6-GDP interaction motif.

Depletion of TRE17 attenuates Arf6 activation. Our data above revealed that overexpression of TRE17(long) or the T17(447) mutant promoted Arf6 activation in vivo. To assess the role of endogenous TRE17(long) in Arf6 activation, we depleted its expression with short interfering RNA. HeLa cells were transfected with a vector encoding a short hairpin sequence modeled after the N terminus of TRE17(long) (T17−). In order to control for nonspecific effects of expressing short double-stranded RNA, we also generated a construct targeting an exon that is absent from the *TRE17* splice variant expressed in HeLa cells. Following transfection, HeLa cells were selected in neomycin and then subjected to reverse transcription-PCR to monitor *TRE17* mRNA levels. As shown in Fig. 10A, *TRE17* expression was essentially abolished in the T17− cells. Strikingly, GGA3 pulldown assays revealed that Arf6 activity was specifically reduced in the T17− cells (Fig. 10B). These data strongly support a role for endogenous TRE17 in promoting Arf6 activation.

DISCUSSION

Our studies identify a role for TRE17 in regulating trafficking through the Arf6-dependent plasma membrane recycling system. Unexpectedly, we find that the TBC domain of TRE17 serves as an Arf6-GDP interaction motif and not as a GAP. Our results are consistent with recent work suggesting that TRE17 is catalytically inactive (7). While it remains formally possible that TRE17 serves as a GAP for a GTPase that we have yet to identify, our mutagenic analysis strongly suggests that GAP activity is not required for TRE17's ability to activate Arf6 or for its effects on the morphology of the tubular endosomal compartment. Interestingly, both TRE17 and PRC17 (TRE17's closest homologue) lack the highly conserved arginine residue that has been shown to function in catalysis in other TBC proteins. However, PRC17 was reported to function as a GAP for Rab5 (49). These results, together with our current findings, underscore the need for caution in predicting the substrate specificity and catalytic mechanism for this poorly characterized family of proteins.

Our studies support a model in which TRE17 promotes Arf6 activation by binding to Arf6-GDP at the tubular endosome and facilitating its recruitment to the plasma membrane, thus bringing it into proximity with its GEFs. An important unanswered question is how TRE17(long) gets recruited to the plasma membrane. Our previous studies indicated that TRE17 is recruited to the membrane by mitogenic stimuli, mediated by an indirect association with Rac1 and Cdc42 (34). Notably, constitutively active Rac1 is sufficient to drive plasma membrane recruitment of both TRE17 (34) and Arf6 (30, 70; our

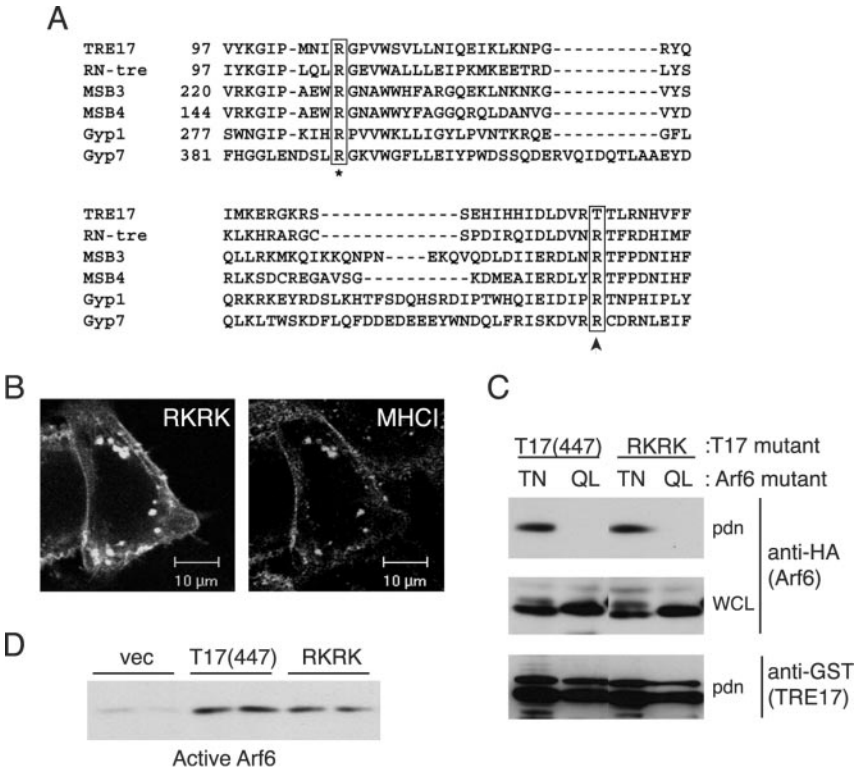

FIG. 9. TRE17 activates Arf6 independently of intrinsic GAP activity. (A) Sequence alignment of TBC proteins; only a portion of the TBC domain is shown. Numbers indicate the amino acid position of the first residue shown. The arginine residue that functions in catalysis is highlighted with an arrow; the corresponding residue in TRE17 is threonine (T150). Another conserved arginine residue required for activity is marked with an asterisk (corresponding to R106 in TRE17). (B) HeLa cells were transfected with a T17(447) mutant in which arginines 106 and 149 were mutated to lysines (RKRK). Live cells were incubated with anti-major histocompatibility complex type I antibody and then processed for indirect immunofluorescence. Scale bar, 10 μm. (C) Wild-type GST-T17(447) or the RKRK mutant was cotransfected with HA-Arf6 Q67L or T27N. T17(447) was precipitated with glutathione-Sepharose, and associated Arf6 was detected by anti-HA immunoblotting. (D) HA-Arf6 was cotransfected with wild-type T17(447) or the RKRK mutant. GGA3 pulldown assays were performed as above. Immunoblotting of whole-cell extracts confirmed uniform expression of the Arf6 and T17(447) mutants (data not shown).

unpublished observations). Thus, it is tempting to speculate that TRE17 serves to link agonist-induced Rac1 activation to enhanced recycling through the Arf6 pathway. Investigating this possibility will be among our future goals.

Following membrane internalization, Arf6 must normally be inactivated by GAPs to allow fusion of endocytic vesicles with the tubular endosome. However, forced expression of TRE17 appears to cause sustained activation of Arf6 on endosomes. In the case of T17(447) this leads to the formation of enlarged vesicles which accumulate cargo. Coexpression of TRE17 (long) with Arf6 similarly causes sustained Arf6 activation, inducing the formation of vacuoles or, less frequently, enlarged vesicles similar to those induced by T17(447). At present, we do not fully understand the molecular basis of these different phenotypes, both of which appear to arise through hyperactivation of Arf6.

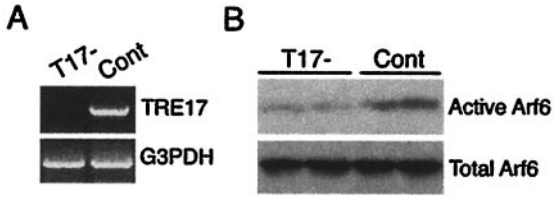

FIG. 10. Arf6 activity is attenuated in HeLa cells depleted of TRE17. (A) HeLa cells were transfected with a construct targeting TRE17 (T17−) or a negative control plasmid (Cont) and then selected in neomycin. RNA was isolated from pooled populations, and reverse transcription-PCR was performed with primers against TRE17 (top panel) or glyceraldehyde-3-phosphate dehydrogenase (bottom panel). (B) T17− and control cells were transfected with HA-Arf6 and then subjected to GGA3 pulldowns.

We believe that the vacuolar phenotype may arise from higher levels of Arf6 activation, based on the fact that Arf6 Q67L induces this morphology (9). We hypothesize that the vacuoles arise from enhanced formation and fusion of pinosomes and macropinosomes, as has been described for Arf6 Q67L (9). In contrast, the enlarged vesicles may result from fusion of endosomes en route to the tubular compartment. The frequent association of the enlarged vesicles with tubules (Fig. 4 and 5) is consistent with such a notion. Because T17(447) lacks the ubiquitin-specific protease domain but was able to induce Arf6 activation, this indicates that TRE17's de-ubiquitinating activity is not absolutely essential for this effect. However, TRE17(onco) was unable to cooperate with wild-type Arf6 in vacuole formation (Fig. 3), suggesting that ubiquitin-specific protease activity may have a modulatory role. Consis-

tent with this notion, a point mutant of TRE17(long) in which ubiquitin-specific protease activity was abolished, TRE17 (long)/USP−, was also unable to cooperate with wild-type Arf6 in vacuole formation (unpublished observations). It may be speculated that TRE17(onco) (which contains only one of the two subdomains required for ubiquitin-specific protease activity) and TRE17(long)/USP− function as dominant negative alleles, being able to bind but not deubiquitinate substrates which regulate either Arf6 activation or vesicle dynamics. In contrast, T17(447), which lacks the entire C terminus, might not function in a dominant negative manner.

While our results indicate that TRE17 induces Arf6 activation by promoting its recruitment to the plasma membrane, we believe that it may have additional functions. This is suggested by the fact that T17(447) and TRE17(long) promote membrane recruitment of Arf6 T27N equally well, but only the former can promote Arf6 activation when expressed by itself (as inferred from effects on endosome morphology). This may reflect the dysregulated nature of T17(447), as suggested by our previous work (34); the putative additional function of TRE17 may be mediated by a domain that is exposed in T17(447) but autoinhibited and subject to regulation in TRE17(long) and TRE17(onco). What might this additional function be? The direct binding of TRE17 to Arf6-GDP raises several possibilities. One is that TRE17 might function as a GEF itself. While we failed to detect intrinsic GEF activity for MBP-T17(447) in in vitro GEF assays (data not shown), future experiments with TRE17 purified from eukaryotic cells will be necessary to eliminate this possibility. Alternatively, TRE17 might directly bridge the interaction of Arf6-GDP with its GEFs, as has been described for β-arrestin (16). Yet another possibility is that binding of TRE17 might alter the conformation of Arf-GDP in a manner that enhances its ability to serve as a GEF substrate. Future studies will examine these potential roles for TRE17 in Arf6 activation.

An outstanding question is the mechanism by which TRE17 causes transformation. Initial studies suggested that TRE17 (onco) was the only isoform capable of causing transformation in NIH 3T3 cells (37). However, more recent studies indicate that TRE17(long) also has tumorigenic properties in vivo. As mentioned, the TRE17 gene undergoes a chromosomal translocation event in bone neoplasms, leading to its high-level expression. TRE17(long) was the only isoform detected in these tumors (A. Oliveira and J. A. Fletcher, personal communication). Since Arf6 has been shown to promote motile, invasive behavior (26, 29, 45, 46, 59, 60, 64), we suggest that this is a key component of TRE17(long)'s mechanism of transformation. In addition, it may be speculated that TRE17 has additional cellular functions that are dependent on ubiquitin-specific protease activity, such as stabilizing proteins (such as tumor suppressors, for example), that are normally targeted for proteasomal or lysosomal degradation. In the case of TRE17(onco)-mediated transformation, degradation of such proteins might be enhanced due to its ability to act in a dominant negative manner. Exploring these possibilities may lead to the identification of novel mechanisms of cellular transformation.

ACKNOWLEDGMENTS

We thank Gerd Blobel, Michael Marks, Christopher Burd, and Erfei Bi for critical comments on the manuscript. Special thanks to Clara Franzini-Armstrong and Nosta Glaser for assistance with immunoelectron microscopy. We also thank Jonathan Fletcher and Andre Oliveira for discussing data prior to publication.

This work was supported by Public Health Service grant CA-81415 from the National Cancer Institute and the Abramson Cancer Center of the University of Pennsylvania Pilot Projects Program.

REFERENCES

1. **Albert, S., and D. Gallwitz.** 1999. Two new members of a family of Ypt/Rab GTPase activating proteins. Promiscuity of substrate recognition. J. Biol. Chem. **274:**33186–33189.
2. **Albert, S., and D. Gallwitz.** 2000. Msb4p, a protein involved in Cdc42p-dependent organization of the actin cytoskeleton, is a Ypt/Rab-specific GAP. Biol. Chem. **381:**453–456.
3. **Albert, S., E. Will, and D. Gallwitz.** 1999. Identification of the catalytic domains and their functionally critical arginine residues of two yeast GTPase-activating proteins specific for Ypt/Rab transport GTPases. EMBO J. **18:**5216–5225.
4. **Ausubel, F. M., R. Brent, R. E. Kingston, D. D. Moore, J. G. Seidman, J. A. Smith, and K. Struhl.** 1997. Curr. Prot. Mol. Biol. II **16**.16.11–16.16.15.
5. **Bernards, A.** 2003. GAPs galore! A survey of putative Ras superfamily GTPase activating proteins in man and Drosophila. Biochim. Biophys. Acta **1603:**47–82.
6. **Bi, E., J. B. Chiavetta, H. Chen, G. C. Chen, C. S. Chan, and J. R. Pringle.** 2000. Identification of novel, evolutionarily conserved Cdc42p-interacting proteins and of redundant pathways linking Cdc24p and Cdc42p to actin polarization in yeast. Mol. Biol. Cell **11:**773–793.
7. **Bizimungu, C., N. De Neve, A. Burny, S. Bach, F. Bontemps, D. Portetelle, and M. Vandenbol.** 2003. Expression in a RabGAP yeast mutant of two human homologues, one of which is an oncogene. Biochem. Biophys. Res. Commun. **310:**498–504.
8. **Boshans, R. L., S. Szanto, L. van Aelst, and C. D'Souza-Schorey.** 2000. ADP-ribosylation factor 6 regulates actin cytoskeleton remodeling in coordination with Rac1 and RhoA. Mol. Cell. Biol. **20**:3685–3694.
9. **Brown, F. D., A. L. Rozelle, H. L. Yin, T. Balla, and J. G. Donaldson.** 2001. Phosphatidylinositol 4,5-bisphosphate and Arf6-regulated membrane traffic. J. Cell Biol. **154:**1007–1017.
10. **Caplan, S., N. Naslavsky, L. M. Hartnell, R. Lodge, R. S. Polishchuk, J. G. Donaldson, and J. S. Bonifacino.** 2002. A tubular EHD1-containing compartment involved in the recycling of major histocompatibility complex class I molecules to the plasma membrane. EMBO J. **21:**2557–2567.
11. **Casanova, J. E.** 2003. ARFs. Curr. Biol. **13:**R123.
12. **Cavenagh, M. M., J. A. Whitney, K. Carroll, C. Zhang, A. L. Boman, A. G. Rosenwald, I. Mellman, and R. A. Kahn.** 1996. Intracellular distribution of Arf proteins in mammalian cells. Arf6 is uniquely localized to the plasma membrane. J. Biol. Chem. **271:**21767–21774.
13. **Chardin, P., S. Paris, B. Antonny, S. Robineau, S. Beraud-Dufour, C. L. Jackson, and M. Chabre.** 1996. A human exchange factor for ARF contains Sec7- and pleckstrin-homology domains. Nature **384:**481–484.
14. **Chavrier, P., and B. Goud.** 1999. The role of ARF and Rab GTPases in membrane transport. Curr. Opin. Cell Biol. **11:**466–475.
15. **Chies, R., L. Nobbio, P. Edomi, A. Schenone, C. Schneider, and C. Brancolini.** 2003. Alterations in the Arf6-regulated plasma membrane endosomal recycling pathway in cells overexpressing the tetraspan protein Gas3/PMP22. J. Cell Sci. **116:**987–999.
16. **Claing, A., W. Chen, W. E. Miller, N. Vitale, J. Moss, R. T. Premont, and R. J. Lefkowitz.** 2001. beta-Arrestin-mediated ADP-ribosylation factor 6 activation and beta 2-adrenergic receptor endocytosis. J. Biol. Chem. **276:**42509–42513.
17. **Collins, R. N.** 2003. Rab and ARF GTPase regulation of exocytosis. Mol. Membr. Biol. **20:**105–115.
18. **Cuif, M. H., F. Possmayer, H. Zander, N. Bordes, F. Jollivet, A. Couedel-Courteille, I. Janoueix-Lerosey, G. Langsley, M. Bornens, and B. Goud.** 1999. Characterization of GAPCenA, a GTPase activating protein for Rab6, part of which associates with the centrosome. EMBO J. **18:**1772–1782.
19. **Dell'Angelica, E. C., R. Puertollano, C. Mullins, R. C. Aguilar, J. D. Vargas, L. M. Hartnell, and J. S. Bonifacino.** 2000. GGAs: a family of ADP ribosylation factor-binding proteins related to adaptors and associated with the Golgi complex. J. Cell Biol. **149:**81–94.
20. **Donaldson, J. G., and C. L. Jackson.** 2000. Regulators and effectors of the ARF GTPases. Curr. Opin. Cell Biol. **12:**475–482.
21. **Donaldson, J. G., and H. Radhakrishna.** 2001. Expression and properties of ADP-ribosylation factor (ARF6) in endocytic pathways. Methods Enzymol. **329:**247–256.
22. **D'Souza-Schorey, C., R. L. Boshans, M. McDonough, P. D. Stahl, and L. Van Aelst.** 1997. A role for POR1, a Rac1-interacting protein, in ARF6-mediated cytoskeletal rearrangements. EMBO J. **16:**5445–5454.

23. **D'Souza-Schorey, C., G. Li, M. I. Colombo, and P. D. Stahl.** 1995. A regulatory role for ARF6 in receptor-mediated endocytosis. Science **267:**1175–1178.
24. **D'Souza-Schorey, C., and P. D. Stahl.** 1995. Myristoylation is required for the intracellular localization and endocytic function of ARF6. Exp. Cell Res. **221:**153–159.
25. **D'Souza-Schorey, C., E. van Donselaar, V. W. Hsu, C. Yang, P. D. Stahl, and P. J. Peters.** 1998. ARF6 targets recycling vesicles to the plasma membrane: insights from an ultrastructural investigation. J. Cell Biol. **140:**603–616.
26. **Franco, M., P. J. Peters, J. Boretto, E. van Donselaar, A. Neri, C. D'Souza-Schorey, and P. Chavrier.** 1999. EFA6, a sec7 domain-containing exchange factor for ARF6, coordinates membrane recycling and actin cytoskeleton organization. EMBO J. **18**:1480–1491.
27. **Frank, S., S. Upender, S. H. Hansen, and J. E. Casanova.** 1998. ARNO is a guanine nucleotide exchange factor for ADP-ribosylation factor 6. J. Biol. Chem. **273:**23–27.
28. **Gao, X. D., S. Albert, S. E. Tcheperegine, C. G. Burd, D. Gallwitz, and E. Bi.** 2003. The GAP activity of Msb3p and Msb4p for the Rab GTPase Sec4p is required for efficient exocytosis and actin organization. J. Cell Biol. **162:**635–646.
29. **Hashimoto, S., Y. Onodera, A. Hashimoto, M. Tanaka, M. Hamaguchi, A. Yamada, and H. Sabe.** 2004. Requirement for Arf6 in breast cancer invasive activities. Proc. Natl. Acad. Sci. USA **101:**6647–6652.
30. **Honda, A., M. Nogami, T. Yokozeki, M. Yamazaki, H. Nakamura, H. Watanabe, K. Kawamoto, K. Nakayama, A. J. Morris, M. A. Frohman, and Y. Kanaho.** 1999. Phosphatidylinositol 4-phosphate 5-kinase alpha is a downstream effector of the small G protein ARF6 in membrane ruffle formation. Cell **99:**521–532.
31. **Jackson, C. L., and J. E. Casanova.** 2000. Turning on ARF: the Sec7 family of guanine-nucleotide-exchange factors. Trends Cell Biol. **10:**60–67.
32. **Langille, S. E., V. Patki, J. K. Klarlund, J. M. Buxton, J. J. Holik, A. Chawla, S. Corvera, and M. P. Czech.** 1999. ADP-ribosylation factor 6 as a target of guanine nucleotide exchange factor GRP1. J. Biol. Chem. **274:**27099–27104.
33. **Lanzetti, L., V. Rybin, M. G. Malabarba, S. Christoforidis, G. Scita, M. Zerial, and P. P. Di Fiore.** 2000. The Eps8 protein coordinates epidermal growth factor receptor signalling through Rac and trafficking through Rab5. Nature **408:**374–377.
34. **Masuda-Robens, J. M., S. N. Kutney, H. Qi, and M. M. Chou.** 2003. The TRE17 oncogene encodes a component of a novel effector pathway for rho GTPases Cdc42 and Rac 1 and stimulates actin remodeling. Mol. Cell. Biol. **23**:2151–2161.
35. **Matoskova, B., W. T. Wong, N. Seki, T. Nagase, N. Nomura, K. C. Robbins, and P. P. Di Fiore.** 1996. RN-tre identifies a family of tre-related proteins displaying a novel potential protein binding domain. Oncogene **12:**2563–2571.
36. **Nagel, W., P. Schilcher, L. Zeitlmann, and W. Kolanus.** 1998. The PH domain and the polybasic c domain of cytohesin-1 cooperate specifically in plasma membrane association and cellular function. Mol. Biol. Cell **9:**1981–1994.
37. **Nakamura, T., J. Hillova, R. Mariage-Samson, M. Onno, K. Huebner, L. A. Cannizzaro, L. Boghosian-Sell, C. M. Croce, and M. Hill.** 1992. A novel transcriptional unit of the tre oncogene widely expressed in human cancer cells. Oncogene **7:**733–741.
38. **Naslavsky, N., R. Weigert, and J. G. Donaldson.** 2003. Convergence of non-clathrin- and clathrin-derived endosomes involves Arf6 inactivation and changes in phosphoinositides. Mol. Biol. Cell **14:**417–431.
39. **Neuwald, A. F.** 1997. A shared domain between a spindle assembly checkpoint protein and Ypt/Rab-specific GTPase-activators. Trends Biochem. Sci. **22:**243–244.
40. **Nie, Z., D. S. Hirsch, and P. A. Randazzo.** 2003. Arf and its many interactors. Curr. Opin. Cell Biol. **15:**396–404.
41. **Niedergang, F., E. Colucci-Guyon, T. Dubois, G. Raposo, and P. Chavrier.** 2003. ADP ribosylation factor 6 is activated and controls membrane delivery during phagocytosis in macrophages. J. Cell Biol. **161:**1143–1150.
42. **Novick, P., and M. Zerial.** 1997. The diversity of Rab proteins in vesicle transport. Curr. Opin. Cell Biol. **9:**496–504.
43. **Oliveira, A. M., B. L. Hsi, S. Weremowicz, A. E. Rosenberg, P. D. Cin, N. Joseph, J. A. Bridge, A. R. Perez-Atayde, and J. A. Fletcher.** 2004. USP6 (Tre2) fusion oncogenes in aneurysmal bone cyst. Cancer Res. **64:**1920–1923.
44. **Palacios, F., and C. D'Souza-Schorey.** 2003. Modulation of Rac1 and ARF6 activation during epithelial cell scattering. J. Biol. Chem. **278**:17395–17400.
45. **Palacios, F., L. Price, J. Schweitzer, J. G. Collard, and C. D'Souza-Schorey.** 2001. An essential role for ARF6-regulated membrane traffic in adherens junction turnover and epithelial cell migration. EMBO J. **20**:4973–4986.
46. **Palacios, F., J. K. Schweitzer, R. L. Boshans, and C. D'Souza-Schorey.** 2002. ARF6-GTP recruits Nm23-H1 to facilitate dynamin-mediated endocytosis during adherens junctions disassembly. Nat. Cell Biol. **4**:929–936.
47. **Papa, F. R., and M. Hochstrasser.** 1993. The yeast DOA4 gene encodes a deubiquitinating enzyme related to a product of the human tre-2 oncogene. Nature **366:**313–319.
48. **Paulding, C. A., M. Ruvolo, and D. A. Haber.** 2003. The Tre2 (USP6) oncogene is a hominoid-specific gene. Proc. Natl. Acad. Sci. USA **100:**2507–2511.
49. **Pei, L., Y. Peng, Y. Yang, X. B. Ling, W. G. Van Eyndhoven, K. C. Nguyen, M. Rubin, T. Hoey, S. Powers, and J. Li.** 2002. PRC17, a novel oncogene encoding a Rab GTPase-activating protein, is amplified in prostate cancer. Cancer Res. **62:**5420–5424.
50. **Peters, P. J., V. W. Hsu, C. E. Ooi, D. Finazzi, S. B. Teal, V. Oorschot, J. G. Donaldson, and R. D. Klausner.** 1995. Overexpression of wild-type and mutant ARF1 and ARF6: distinct perturbations of nonoverlapping membrane compartments. J. Cell Biol. **128:**1003–1017.
51. **Powelka, A. M., J. Sun, J. Li, M. Gao, L. M. Shaw, A. Sonnenberg, and V. W. Hsu.** 2004. Stimulation-dependent recycling of integrin b1 regulating by Arf6 and Rab11. Traffic **5:**20–36.
52. **Radhakrishna, H., O. Al-Awar, Z. Khachikian, and J. G. Donaldson.** 1999. ARF6 requirement for Rac ruffling suggests a role for membrane trafficking in cortical actin rearrangements. J. Cell Sci. **112:**855–866.
53. **Radhakrishna, H., and J. G. Donaldson.** 1997. ADP-ribosylation factor 6 regulates a novel plasma membrane recycling pathway. J. Cell Biol. **139:**49–61.
54. **Radhakrishna, H., R. D. Klausner, and J. G. Donaldson.** 1996. Aluminum fluoride stimulates surface protrusions in cells overexpressing the ARF6 GTPase. J. Cell Biol. **134:**935–947.
55. **Rak, A., R. Fedorov, K. Alexandrov, S. Albert, R. S. Goody, D. Gallwitz, and A. J. Scheidig.** 2000. Crystal structure of the GAP domain of Gyp1p: first insights into interaction with Ypt/Rab proteins. EMBO J. **19:**5105–5113.
56. **Randazzo, P. A., and H. M. Fales.** 2002. Preparation of myristoylated Arf1 and Arf6 proteins. Methods Mol. Biol. **189:**169–179.
57. **Randazzo, P. A., Z. Nie, K. Miura, and V. W. Hsu.** 2000. Molecular aspects of the cellular activities of ADP-ribosylation factors. Sci. STKE **2000**(59): RE1. [Online.]
58. **Richardson, P. M., and L. I. Zon.** 1995. Molecular cloning of a cDNA with a novel domain present in the tre-2 oncogene and the yeast cell cycle regulators BUB2 and cdc16. Oncogene **11:**1139–1148.
59. **Santy, L. C.** 2002. Characterization of a fast cycling ADP-ribosylation factor 6 mutant. J. Biol. Chem. **277:**40185–40188.
60. **Santy, L. C., and J. E. Casanova.** 2001. Activation of ARF6 by ARNO stimulates epithelial cell migration through downstream activation of both Rac1 and phospholipase D. J. Cell Biol. **154:**599–610.
61. **Schwoebel, E. D., T. H. Ho, and M. S. Moore.** 2002. The mechanism of inhibition of Ran-dependent nuclear transport by cellular ATP depletion. J. Cell Biol. **157:**963–974.
62. **Song, J., Z. Khachikian, H. Radhakrishna, and J. G. Donaldson.** 1998. Localization of endogenous ARF6 to sites of cortical actin rearrangement and involvement of ARF6 in cell spreading. J. Cell Sci. **111:**2257–2267.
63. **Strom, M., P. Vollmer, T. J. Tan, and D. Gallwitz.** 1993. A yeast GTPase-activating protein that interacts specifically with a member of the Ypt/Rab family. Nature **361:**736–739.
64. **Tague, S. E., V. Muralidharan, and C. D'Souza-Schorey.** 2004. Arf6 regulates tumor cell invasion via the activation of the MEK/Erk signaling pathway. Proc. Natl. Acad. Sci. USA **101:**9671–9676.
65. **Takatsu, H., K. Yoshino, K. Toda, and K. Nakayama.** 2002. GGA proteins associate with Golgi membranes through interaction between their GGAH domains and ADP-ribosylation factors. Biochem. J. **365:**369–378.
66. **Tan, T. J., P. Vollmer, and D. Gallwitz.** 1991. Identification and partial purification of GTPase-activating proteins from yeast and mammalian cells that preferentially act on Ypt1/Rab1 proteins. FEBS Lett. **291:**322–326.
67. **Venkateswarlu, K., F. Gunn-Moore, P. B. Oatey, J. M. Tavare, and P. J. Cullen.** 1998. Nerve growth factor- and epidermal growth factor-stimulated translocation of the ADP-ribosylation factor-exchange factor GRP1 to the plasma membrane of PC12 cells requires activation of phosphatidylinositol 3-kinase and the GRP1 pleckstrin homology domain. Biochem. J. **335:**139–146.
68. **Venkateswarlu, K., P. B. Oatey, J. M. Tavare, and P. J. Cullen.** 1998. Insulin-dependent translocation of ARNO to the plasma membrane of adipocytes requires phosphatidylinositol 3-kinase. Curr. Biol. **8:**463–466.
69. **Vollmer, P., and D. Gallwitz.** 1995. High expression cloning, purification, and assay of Ypt-GTPase-activating proteins. Methods Enzymol. **257:**118–128.
70. **Zhang, Q., J. Calafat, H. Janssen, and S. Greenberg.** 1999. ARF6 is required for growth factor- and Rac-mediated membrane ruffling in macrophages at a stage distal to Rac membrane targeting. Mol. Cell. Biol. **19:**8158–8168.
71. **Zhang, Q., D. Cox, C. C. Tseng, J. G. Donaldson, and S. Greenberg.** 1998. A requirement for ARF6 in Fcgamma receptor-mediated phagocytosis in macrophages. J. Biol. Chem. **273:**19977–19981.
72. **Zhang, S. D., J. Kassis, B. Olde, D. M. Mellerick, and W. F. Odenwald.** 1996. Pollux, a novel Drosophila adhesion molecule, belongs to a family of proteins expressed in plants, yeast, nematodes, and man. Genes Dev. **10:**1108–1119.